



ELSEVIER

Available online at www.sciencedirect.com

SCIENCE @ DIRECT®

Physica A 325 (2003) 577–600

PHYSICA A

www.elsevier.com/locate/physa

Continuum percolation of wireless ad hoc communication networks

Ingmar Glauche^{a,b,*}, Wolfram Krause^{a,c}, Rudolf Sollacher^a,
Martin Greiner^a

^aCorporate Technology, Information & Communications, Siemens AG, D-81730 München, Germany

^bInstitut für Theoretische Physik, Technische Universität, D-01062 Dresden, Germany

^cInstitut für Theoretische Physik, Johann Wolfgang Goethe-Universität, Postfach 11 19 32,
D-60054 Frankfurt am Main, Germany

Received 25 October 2002

Abstract

Wireless multi-hop ad hoc communication networks represent an infrastructure-less and self-organized generalization of today's wireless cellular networks. Connectivity within such a network is an important issue. Continuum percolation and technology-driven mutations thereof allow to address this issue in the static limit and to construct a simple distributed protocol, guaranteeing strong connectivity almost surely and independently of various typical uncorrelated and correlated random spatial patterns of participating ad hoc nodes.

© 2003 Elsevier Science B.V. All rights reserved.

PACS: 05.40.+j; 64.60.Ak; 02.40.Pc; 84.40.Ua; 89.20.+a; 89.80.+h

Keywords: Continuum percolation; Random geometric graphs; Wireless ad hoc networks; Information and communication technology

1. Introduction

Today's wireless communication mainly relies on cellular networks [1–3]. At first, the sending mobile device directly connects to its nearest base station. A backbone network then routes the communication packets to the cell, where the intended receiving

* Corresponding author. Institut für Theoretische Physik, Technische Universität Dresden, Dresden 01062, Germany.

E-mail addresses: glauche@physik.phy.tu-dresden.de (I. Glauche), krause@th.physik.uni-frankfurt.de (W. Krause), rudolf.sollacher@siemens.com (R. Sollacher), martin.greiner@siemens.com (M. Greiner).

mobile device is registered. Finally, the cell's base station transmits the passed-by message to the latter. As part of the centralized backbone infrastructure each base station acts as a router, possesses the network information, controls the single-hop communications within its cell and assigns different channels to its various mobile clients. The base stations need to be placed according to some optimized coverage layout. This requires an enormous planning effort ahead of operation and leads to a static infrastructure, hard to change and adapt to new, revised needs. This costly inflexibility motivates a flexible and infrastructure-less peer-to-peer concept: selforganizing wireless mobile ad hoc networks [4–7].

In a wireless ad hoc network, a sending mobile device uses inbetween mobile devices to communicate with the intended receiver. Such a multi-hop connection requires each mobile device to have additional router functionality. As a central control authority is missing, the participating devices need coordination amongst themselves to ensure network connectivity, efficient discovery and execution of end-to-end routes and avoidance of data packet collisions on shared radio channels; of course, mobility of the devices also has an impact on the network performance, which has to be coped with. Contrary to these global network features, the selforganizing coordination rules, called protocols in the jargon of electrical engineers, have to be local. Due to its limited transmission range, a mobile device is able to communicate only with its current spatial neighbors. Hence, it can only extract information on its local surrounding. Since this is the only input into the coordination rule, the latter is by definition local. Upon execution, it readjusts for example the device's transmission power to its new surrounding.

In this paper we focus on the important connectivity issue and ask: what is a good local coordination rule for transmission power management, which almost surely guarantees global connectivity for the whole network? We employ a simple static model for ad hoc communication networks. This allows a connection to continuum percolation theory [8,9] based on random geometric graphs [10,11]. The spatially distributed ad hoc devices correspond to nodes, which are more or less locally connected by communication links. Two nodes establish a mutual link, only if the first node lies within the transmission range of the second and vice versa. For the case of constant, isotropic transmission ranges, a further mapping onto the classical picture of continuum percolation [12,13], stemming from the transport physics in continuous random media, is straightforward: whenever discs with radius equaling half of the transmission range are placed around two nodes and overlap, the two nodes are linked.

Continuum percolation allows to study, for example, the dependence of the probability for strong connectivity on the transmission range and to find a critical range, above which the ad hoc network graph is almost surely connected. The critical transmission range can be translated into a critical node neighborhood degree ngb_{crit} . Hence, a simple local coordination rule would be for each node to adjust its transmission power to yield a little above ngb_{crit} neighbors. As we will demonstrate, such a rule is not flexible enough to perform equally well in various different environments, like homogeneous vs. heterogeneous random spatial arrangements of nodes or homogeneous vs. heterogeneous propagation media. Fortunately, such a rule is able to give some guidance to develop local coordination rules with improved adaptation properties. In some respect, these new rules represent technology-driven mutations of the

continuum percolation problem and demonstrate the usefulness to combine real-world needs in electrical engineering with modified concepts of statistical physics.

In Section 2 a precise definition of random geometric graphs in the context of wireless ad hoc communication networks is given; various spatial point patterns, uncorrelated and correlated, are introduced. In Section 3 standard continuum percolation based on discs with constant and random radius is applied to ad hoc networks to obtain first rigorous statements on coordination rules for connectivity. A mutation of continuum percolation is presented in Section 4, which directly leads to a distributed, local coordination rule, flexible enough to cope with various environments. A conclusion and outlook is given in Section 5.

2. Random geometric graph approach to ad hoc networks

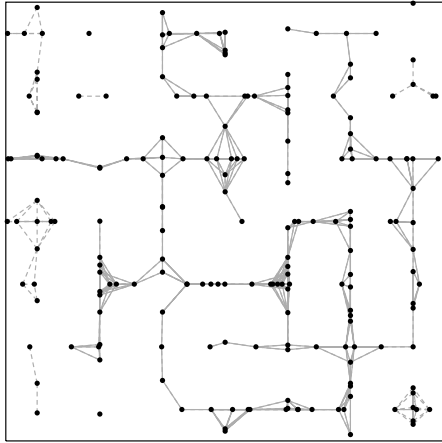
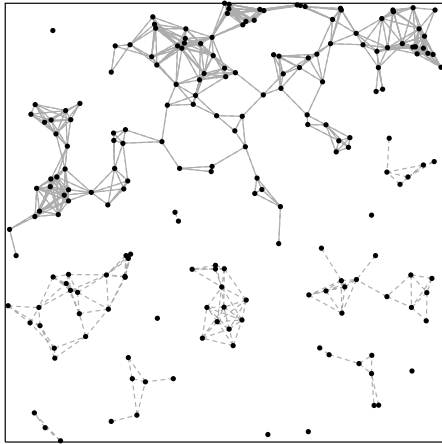
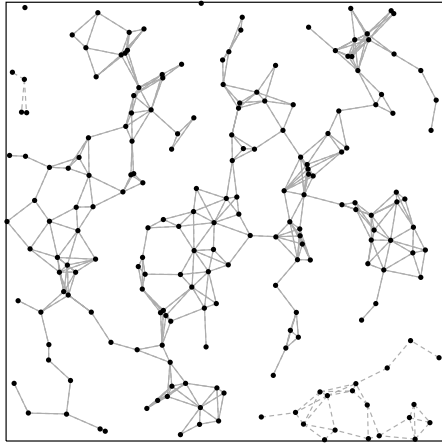
The topology of static ad hoc networks can be viewed as a random geometric graph. It consists of a spatial pattern of points, where each point is connected to some others by links. In Section 2.1 the construction of three generic random point patterns is described. A simple propagation-receiver model is used in Section 2.2 to establish links between points. Some selected geometric-graph features of interest are discussed in Section 2.3.

2.1. Spatial point patterns

Throughout this paper three different generic random spatial point patterns are used: a homogeneous, a multifractal and a Manhattan point pattern. In the following comes a short description of their construction. With no loss of generality a two-dimensional square area with side length $L = 1$ is used.

In a random homogeneous point pattern each of the N points is given a random position $(x, y) \in [0, L] \times [0, L]$. A typical realization is illustrated in Fig. 1a. By definition it does not show generic clustering.

One way to construct simple clustered point patterns is to employ a binary multiplicative branching process. The nonuniform probability measure supported on the unit square is constructed by iteration: at first the parent square is divided into four offspring squares with area $\frac{1}{4}$. Two randomly chosen offsprings get a fraction $(1 + \beta)/4$ of the parent probability mass $\mu = 1$, whereas the remaining two get a fraction $(1 - \beta)/4$. In the next iteration step each offspring square follows the same probabilistic branching rule and nonuniformly redistributes its probability mass onto its own four offsprings. After j iteration steps the probability mass $\mu = 1$ has been nonuniformly subdivided onto 4^j subsquares with area $1/4^j$, where $\binom{j}{i} 2^i$ of these subsquares ($0 \leq i \leq j$) come with probability mass $[(1 + \beta)/4]^i [(1 - \beta)/4]^{j-i}$. One after the other each of the N points to be distributed is given an independent and uniform random number between 0 and 1, which, given some probability-mass-weighted ordering of the 4^j subsquares, corresponds to exactly one subsquare, onto the particle is deposited and randomly placed inside. One such realization of a point pattern is shown in Fig. 1b. The hierarchical clustering of points is due to the hierarchical branching structure of the iteration process.



The probability measure constructed with such a multiplicative branching process is a multifractal [14]. The construction of multifractal fields has some importance in such diverse fields as turbulence [15–18], finance [19,20], Internet traffic [21], high-energetic multiparticle dynamics [22] and deterministic chaos [23], just to name a few.

As a third generic class of spatial point patterns a Manhattan street pattern is used. N_x and N_y streets are equidistantly placed parallel to the x - and y -axis, respectively. One after the other each of the N points is randomly placed onto one randomly chosen street. Fig. 1c gives an illustration of one realization.

2.2. Construction of communication links

For a wireless communication network we define a link between two nodes i and j , only if they can communicate back and forth to each other. Let $P = P_i$ denote the transmission power given to node i , then according to a simple propagation-receiver model, which does not account for shadowing and fast-fading effects, node j is able to receive the signal once

$$\frac{P/r^\alpha}{noise} \geq snr. \quad (1)$$

$r = r_{ij}$ is the relative Euclidean distance between nodes i and j . The path-loss exponent α is assumed to be constant; for free-space propagation it is $\alpha = 2$, but depending on specific in-/outdoor propagation it can vary typically between $1 \leq \alpha \leq 6$. For a successful signal transmission the received power P_i/r_{ij}^α relative to a noise power needs to be larger than the minimum signal-to-noise ratio snr . Without any loss of generality the variables $noise$ and snr can be set equal to one, implying a rescaling of the power P_i . Condition (1) guarantees that node j is able to hear node i . This alone would define a directed link $i \rightarrow j$. Since bidirectionality increases the efficiency of the communication feedback, we focus on bidirectional links ($i \leftrightarrow j$): also i needs to hear j , implying that also (1) has to be fulfilled with the substitution $P_i \rightarrow P_j$. We call a bidirectional link a communication link.

The link construction can be given a simple geometric interpretation. With $P = P_i$ the condition (1) translates into a maximum range $R_i = P_i^{1/\alpha}$. Nodes that lie inside this circle with radius R_i around node i are able to hear this node. For a communication link to exist between nodes i and j , j has to lie inside i 's circle with radius R_i and i has to lie inside j 's circle with radius R_j . For the case that all $R_i = R$ are identical, this link construction matches the standard link construction of continuum percolation [12].

Besides various spatial point patterns Fig. 1 also illustrates the communication links. Each node has been given identical power $P/P_{norm} = 5$, where the normalization

Fig. 1. Geometric graphs for random patterns of $N = 200$ points confined to a box: homogeneous (top), multifractal (middle) and Manhattan (bottom). Parameters of the point patterns are $j=5$, $\beta=0.4$ (multifractal) and $N_x = N_y = 7$ (Manhattan). Each point is given the same transmission power $P/P_{norm} = 5$, corresponding to a link range $R/L = 0.089$ when using the path-loss exponent $\alpha = 2$. Points connected by solid links belong to the giant-component cluster.

$P_{\text{norm}} = R_{\text{norm}}^z$ comes by setting $\pi R_{\text{norm}}^2 = L^2/N = 1/\rho$ equal to the reciprocal of the node density ρ . Note that no periodic boundary conditions have been used for this figure.

2.3. Geometric-graph features of interest

In Sections 3 and 4 various rules for assigning power values to the ad hoc nodes will be discussed. Each such rule together with a chosen generic class of spatial point patterns defines a specific ensemble of geometric graphs. For example, the graphs of Figs. 1a–c each represent one realization out of three different ensembles: (a) identical power for a random homogeneous spatial point pattern, (b) identical power for a multifractally clustered random spatial point pattern, and (c) identical power for a Manhattan random spatial point pattern.

One question to ask for each ensemble of geometric graphs is for example: how large is the average giant component? The giant component is defined as the magnitude of the largest connected cluster appearing in a graph realization; see again Fig. 1 for a visualization. A related and important question to ask for ad hoc communication networks is, what is the probability that all nodes are able to communicate to each other via multihop link routes? With other words, what is the probability that the giant component is equal to the number of nodes N ? As connectivity is for sure a very important issue for ad hoc communication networks, so is a generalization called k -connectivity. A graph is called k -connected if between every pair of nodes there exist at least k independent paths, which implies, that once $k - 1$ nodes are removed at random, the graph remains at least one-connected. A k -connected ad hoc communication network is more flexible and robust to routing failure. Hence, another question: what is the probability for an ad hoc geometric graph to be k -connected?

A simple flooding algorithm is used to determine the giant component of an ad hoc graph realization: a random node is tagged in first place, then its neighbors are tagged, which then continue to tag their untagged neighbors, and so on, until the corresponding cluster is saturated. This procedure is repeated for all untagged nodes, until all nodes of the graph are tagged. By definition, the largest found cluster is equal to the giant component. For an ad hoc geometric graph to be one-connected, i.e., strongly connected, the giant component has to equal the total number of nodes. Another procedure to inquire one-connectivity uses the $N \times N$ Laplace matrix [24], which is the difference between the diagonal node degree matrix and the adjacency matrix. An element of the adjacency matrix is either one or zero, depending on whether a link does or does not exist between the two respective nodes; a diagonal element of the node degree matrix counts the link neighbors of the respective node. If the Laplace matrix possesses only one zero eigenvalue, then the graph is one-connected; the number of zero eigenvalues counts the number of partitioned clusters. We have employed the Laplace matrix algorithm only as a supplement for small N geometric graphs. The probability for one-connectivity is estimated from a representative sample of ad hoc geometric graph realizations as the ratio between one-connected and all sample graphs.

$(k > 1)$ -connectivity is algorithmically very costly. In a nutshell, for each of the $N(N - 1)/2$ pair of nodes belonging to one graph it has to be checked whether at least k independent paths exist. Although some faster, but approximate algorithms can

be found in the recent literature [25], we prefer to switch from costly k - to cheap pseudo- k -connectivity. Given one-connectivity, the latter only requires each node to have at least k neighbors. In fact, a theorem exists [26], which, translated into our language, guarantees for a geometric graph ensemble based on random homogeneous point patterns and the artificial constant-power link rule of Section 3.1 that in the large N limit the probabilities for k - and pseudo- k -connectivity converge as they approach one.

3. Continuum percolation with artificial link rules

3.1. Artificial link rule I: constant transmission power

The simplest rule for power assignment is to allocate the same power value $P_i = P$ to each node i . This is an artificial and unrealistic rule. It would require all nodes either to be designed for only the same single-valued power operation or, given already network connectivity, to carry out fast synchronization; of course, also an outside provider could adjust all node powers to one single value, but this would give up the infrastructureless philosophy of ad hoc networks. Nevertheless, the constant- P rule is good to start with [27].

Fig. 2 shows the average relative giant component as a function of P obtained from a sample of 500 geometric graphs generated with random homogeneous spatial point patterns and the constant- P rule. The chosen rather small sample size produces already more than sufficient statistical convergence and keeps statistical error bars to such small values, that those will not be shown for this and the following figures. A percolation threshold behavior around $P_{\text{crit}} \approx 4.5P_{\text{norm}}$ is observed: for $P \ll P_{\text{crit}}$ the average relative giant component is close to zero, whereas for $P \gg P_{\text{crit}}$ it is almost equal to one. The sharpness of the threshold depends on the number of participating nodes; with increasing N the transition becomes sharper.

For the determination of the exact threshold position the limit $N \rightarrow \infty$ would be needed. To partially account for this, the relative giant component has also been determined from small and medium N simulations with periodic boundary conditions. Results are also shown in Fig. 2. The percolation transition becomes sharper and moves a little to the left once compared with the previous results, but still no full convergence for the employed increasing N values is obtained. Since for realistic ad hoc networks the limit $N \rightarrow \infty$ is out of reach, we do not pursue this matter further. For the rest of this paper we focus on $N = 1600$, which accommodates best a hot-spot, i.e., big-crowd application of wireless ad hoc networks.

The critical power $P_{\text{crit}} \approx 4.5P_{\text{norm}}$, obtained by setting the path-loss exponent equal to $\alpha = 2$, can be given a more illustrative interpretation: the factor 4.5 reflects the average number of neighboring nodes, which is also denoted as the average node degree. Defining $P_{\text{crit}} = R_{\text{crit}}^2$ along the lines of relation (1), we get $\langle k \rangle = \pi R_{\text{crit}}^2 \rho \approx 4.5\pi R_{\text{norm}}^2 \rho = 4.5$. Picking one node, the probability to find k other nodes inside its circular disc with radius R_{crit} is equal to $p(k) = \binom{N-1}{k} q^k (1-q)^{N-1-k} \approx (\lambda^k / k!) e^{-\lambda}$, where $q = \pi R_{\text{crit}}^2 / L^2$. For N large and q small, $p(k)$ becomes a Poissonian with mean

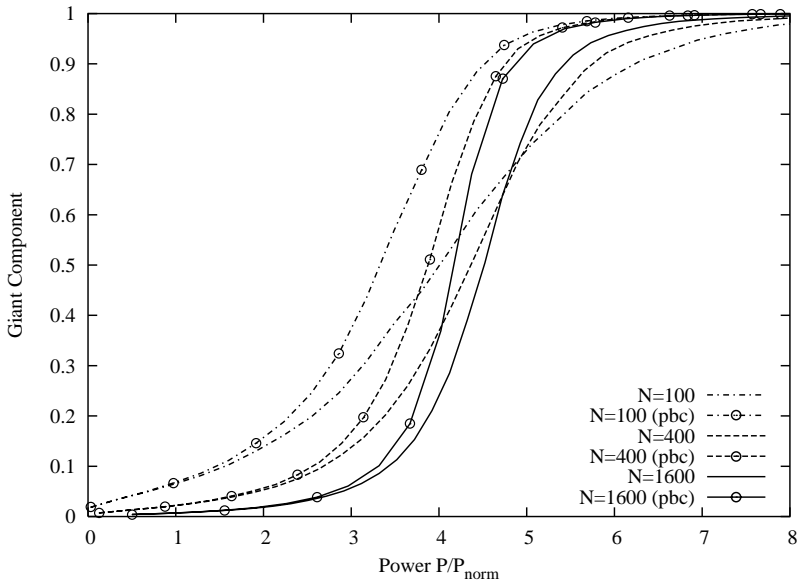


Fig. 2. Average relative giant component as a function of transmission power. A sample of 500 geometric graphs generated with random homogeneous spatial point patterns and the constant- P rule has been used. The path-loss exponent of Eq. (1) has been set to $\alpha=2$. Different curves correspond to different number of nodes: $N = 100$ (dash-dotted), 400 (dashed), 1600 (solid); curves marked without/with open circles correspond to exclusion/inclusion of periodic boundary conditions (pbc).

$\langle k \rangle = \lambda = q(N - 1) \approx qN \approx 4.5$. Note, that due to finite-size effects and the usage of no periodic boundary conditions the actually sampled critical link degree is a little smaller than the asymptotic value $k_{\text{crit}} = 4.53$, which is stated for example in Ref. [10]. This demonstrates that other than in terms of P_{crit} it is also convenient to characterize the percolation phase transition in terms of R_{crit} or k_{crit} . Once choosing other path-loss exponents $\alpha \neq 2$, the former will change according to $P_{\text{crit}}(\alpha \neq 2) = R_{\text{crit}}^{\alpha-2} P_{\text{crit}}(\alpha = 2)$, whereas R_{crit} or k_{crit} remain as before.

Next, spatial point patterns other than random homogeneous are discussed. Fig. 3 compares the relative average giant component as a function of transmission power obtained for random multifractal and Manhattan spatial point patterns with the random homogeneous case; consult again Fig. 1.

Evidently for small P the relative giant component is larger for the multifractal than for the homogeneous patterns, but for the convergence of the relative giant component towards one a much larger P is needed. Due to the hierarchical clustering, subclusters of points are easily formed at small P since only a small transmission range is needed to connect the corresponding nodes. However, in order to connect the various subclusters either directly to each other or via isolated nodes lying inbetween it needs a rather large power. Another consequence of the pronounced clustering is that the rather sharp percolation threshold observed for homogeneous point patterns blurs more the larger the splitting parameter β characterizing the multifractal point patterns is chosen.

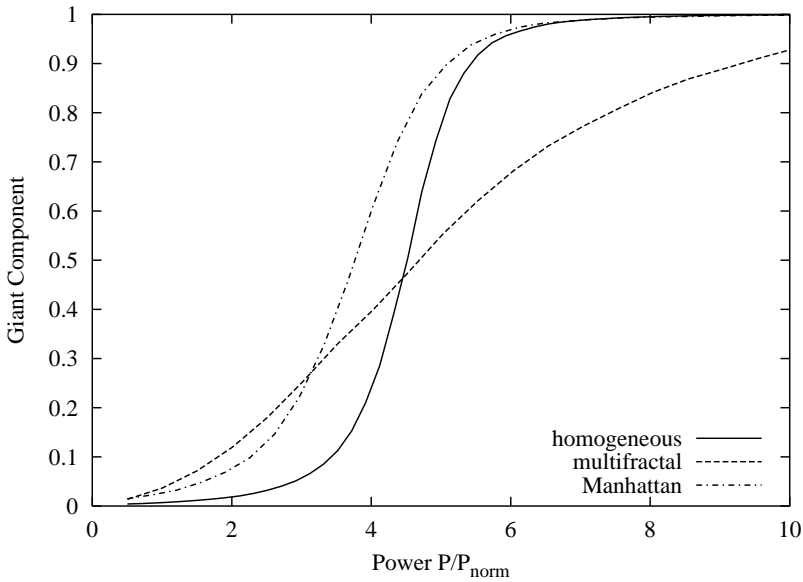


Fig. 3. Average relative giant component as a function of transmission power upon using the constant- P rule. The number of nodes has been fixed to $N = 1600$ and the path-loss exponent has been set to $\alpha = 2$. Different curves correspond to different random spatial patterns: homogeneous (solid), multifractal (dashed) with parameters $\beta = 0.4$ and $j = 5$, and Manhattan (dash-dotted) with parameters $N_x = N_y = 7$. A sample of 500 geometric graphs has been used for each case.

Also for the Manhattan point patterns the relative giant component increases faster for small transmission powers than for the homogeneous point patterns. The reason is that the average nearest-point distance is smaller for the random points confined to the one-dimensional Manhattan streets. The Manhattan threshold for the relative giant component is relatively sharp and comes at a transmission power value, which is somewhat smaller than for random homogeneous point patterns. For consistency, it is instructive to map the continuum percolation based on random Manhattan point patterns onto the well-known square-lattice bond percolation [29]. Two nodes are assumed to lie on a one-dimensional straight line and to have a distance $l = L/N_x = L/N_y$, corresponding to the distance of two successive Manhattan street crossings. They can only communicate with each other, if inbetween nodes come with successive distances x smaller than their transmission range R ; otherwise the occurring void is too large to be bridged. For a one-dimensional Poissonian point pattern with density $\lambda = N/(N_x + N_y)$ the distance x of two consecutive nodes is exponentially distributed according to $p(x) = \lambda \exp(-\lambda x)$. This allows to estimate the probability for the occurrence of at least one too large void between the two picked nodes with distance l . The expression is

$$p(\text{void} > R) = \sum_{j=1}^m \frac{(-\lambda)^{j-1}}{(j-1)!} (l - jR)^{j-1} \left[1 + \frac{\lambda}{j} (l - jR) \right] e^{-j\lambda R}, \quad (2)$$

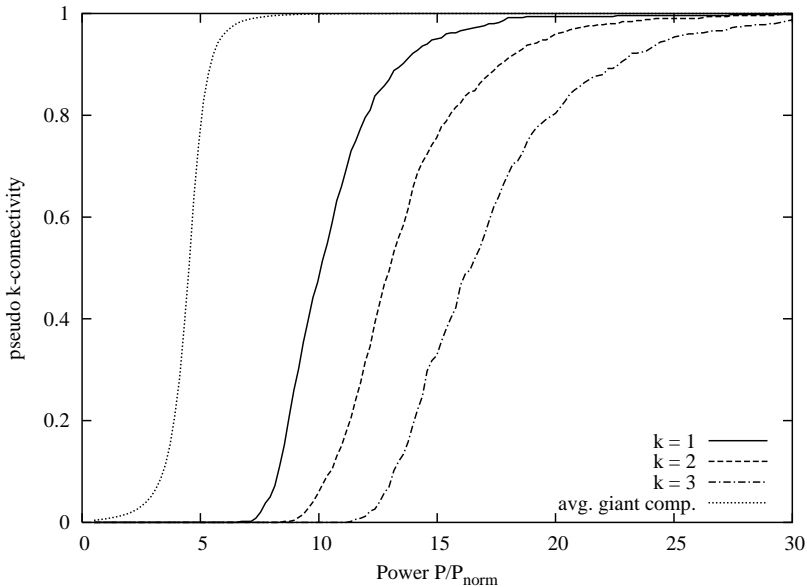


Fig. 4. Probability of pseudo k -connectivity as a function of transmission power upon using the constant- P rule. The number of nodes for the simulated 500 random homogeneous point patterns has been fixed to $N = 1600$ and the path-loss exponent has been set to $\alpha = 2$. Different curves correspond to $k = 1$ (solid), 2 (dashed), 3 (dash-dotted); for comparison the average relative giant component is shown as the dotted curve.

where $m = \lfloor 1/R \rfloor$; a derivation of this formula is given for example in Ref. [28]. Setting the path-loss exponent to $\alpha = 2$ and according to (1) converting the threshold power $P \approx 4P_{\text{norm}}$ into R we arrive at a value $p(\text{void} > R) = 0.47$, which almost matches the critical bond probability $p_{\text{bond}} = 0.50$ of bond percolation on a square lattice [29].

As long as the average relative giant component is not exactly one, no direct knowledge on the probability for strong connectivity, i.e., one-connectivity, is possible. The ($k = 1$) curve of Fig. 4 illustrates this quantity as a function of P obtained from a sample of 500 geometric graphs generated with random homogeneous spatial point patterns and the constant- P rule. It also reveals a threshold behavior, which sets in once the relative giant component has approached one. The relative factor of the respective threshold positions is about 2.3. The probabilities for pseudo- k connectivity with $k = 2$ and 3 are also depicted in Fig. 4. Of course, their threshold is shifted to even larger P when compared to the pseudo-one threshold. A part of Fig. 5 shows the probability for strong connectivity for random multifractal and Manhattan point patterns. Whereas the Manhattan curve is close to the homogeneous curve, the onset for a nonvanishing probability in case of the multifractal point patterns is shifted to extremely large values of the transmission power. This is due to the inhomogeneous spatial clustering and demonstrates that the constant- P rule is not efficient in such an environment.

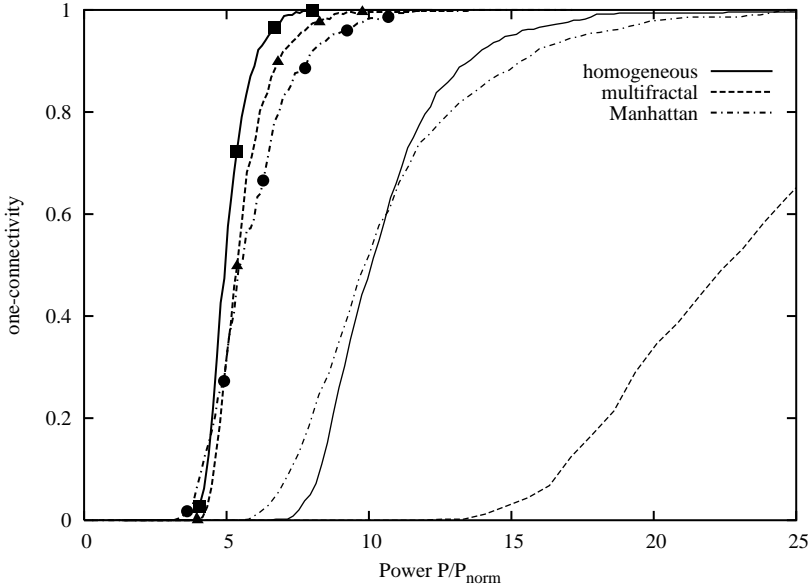


Fig. 5. Probability for one-connectivity as a function of average transmission power upon using the local minimum-link-degree rule (curves with symbols) and the artificial constant- P rule (curves without symbols). The number of nodes has been fixed to $N = 1600$ and the path-loss exponent has been set to $\alpha = 2$. Different line types of the curves correspond to different random spatial point patterns: homogeneous (solid), multifractal (dashed) with parameters $\beta = 0.4$ and $j = 5$, Manhattan (dash-dotted) with parameters $N_x = N_y = 7$; a sample of 500 geometric graphs has been used for each case. From the left to the right the symbols on each minimum-link-degree-rule curve stand for $n_{gh_{\min}} = 3-6$ (homogeneous), $3-7$ (multifractal) and $5-10$ (Manhattan).

3.2. Artificial link rule II: iid transmission power

So far all nodes were assigned the same transmission power P . This constant- P rule is not able to counterbalance spatially sparse regions, which remain disconnected to the giant component. Some long-range links are called for to establish connections between otherwise separated subclusters. Some ad hoc nodes then have to send with a transmission power larger than average. The simplest heterogeneous rule in this context is the iid- P link rule [30]. It treats the transmission power values assigned to the ad hoc nodes as independently and identically distributed (iid) random variables. Independently from the other nodes each node chooses its power according to the same probability distribution $p(P)$ with mean $\langle P \rangle$. Translating P into a transmission range R , this rule places a disc with random radius R around each node.

As a flexible representative a bimodal distribution

$$p(P) = \frac{\beta_2}{\beta_1 + \beta_2} \delta(P - \langle P \rangle(1 - \beta_1)) + \frac{\beta_1}{\beta_1 + \beta_2} \delta(P - \langle P \rangle(1 + \beta_2)) \quad (3)$$

is chosen. It comes with two parameters β_1 and β_2 determining the variance and skewness of this distribution, but leaving the mean $\langle P \rangle$ untouched. The previously

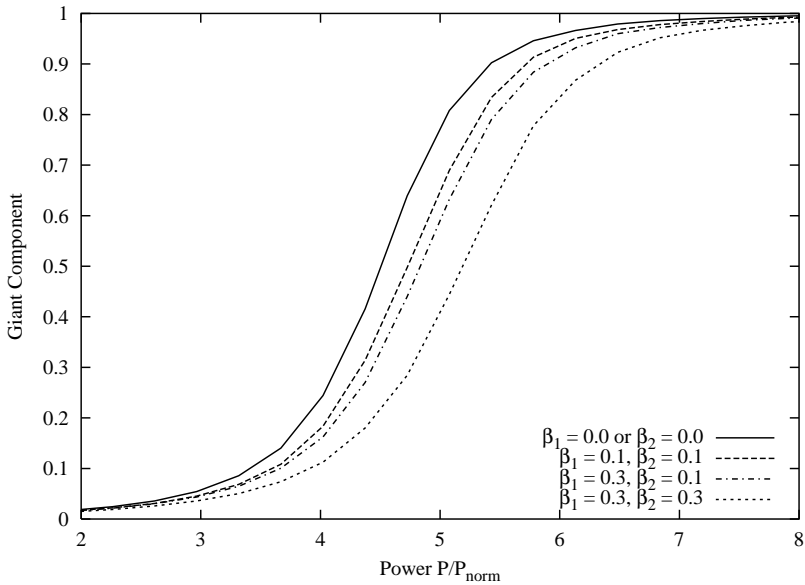


Fig. 6. Average relative giant component as a function of the average transmission power upon using the iid- P rule. The number of nodes for each of the used 500 random homogeneous point patterns has been fixed to $N = 1600$ and the path-loss exponent has been set to $\alpha = 2$. Different curves correspond to different parameter choices: $\beta_1, \beta_2 = 0.0, 0.0$ (solid, constant- P rule), 0.1, 0.1 (dashed), 0.3, 0.1 (dash-dotted), 0.3, 0.3 (dotted).

used constant- P rule is reproduced once $\beta_1 = 0$ or $\beta_2 = 0$. Fig. 6 illustrates simulation results obtained with random homogeneous point patterns. The relative giant component as a function of the average transmission power $\langle P \rangle$ is shown for some combinations of β_1 and β_2 . All settings result in a shift of the percolation threshold to larger $\langle P \rangle$ values when compared to the outcome of the constant- P rule. Without showing we remark that similar results are obtained for other point patterns, i.e., multifractal or Manhattan, and other power distributions, e.g. of lognormal type. The randomness and spatial decorrelation of the long-range links introduced by the iid- P link rule does not allow for a shift of the percolation threshold towards smaller $\langle P \rangle$ values. In the next Section a much more elegant and spatially correlated approach is found to achieve this goal.

4. Continuum percolation with a local link rule

Since a central control authority does not exist in pure ad hoc networks, there is no external provider to assign specific power values to the ad hoc nodes according to its global rule. It is the ad hoc network by itself which has to decide which power values are assigned to its participating nodes. Due to the finite communication range of each

node, see again Eq. (1), these coordination rules have to be local. In the jargon of electrical engineers local means distributed. Such a local rule will be presented and discussed in this section.

4.1. Local link rule: minimum degree

By exchanging so-called hello and hello-reply messages each ad hoc node is able to access direct information only from its immediate neighbors, defined by its links. The simplest local observable for a node is the number of its links, which is equal to the number of its one-hop neighbors. Based on this observable alone, a simple strategy for a node would be to decrease/increase its transmission power once it has more/less than enough neighbors [31]. Consequently the target node degree would be confined between a lower and upper bound \underline{ngb} and \overline{ngb} ; for simplicity of the following arguments we set $\underline{ngb} = \overline{ngb} = ngb$. A value of the latter has to be chosen such that for example almost all nodes are part of one connected network and reflects the only external input to this otherwise local link rule. For example, the results of the previous Section obtained with random homogeneous point patterns suggest, that in order to guarantee a probability almost equal to one for one-connectivity the target value should be of the order $O(ngb) \approx 15\text{--}20$; consult again Fig. 4 and note, that according to the argument given in Section 3.1 in conjunction with random homogeneously distributed point patterns and a path-loss exponent $\alpha = 2$, the relative transmission power P/P_{norm} can be interpreted as the average number of node neighbors.

This simple ngb local link rule has at least two drawbacks. The target range $O(ngb) \approx 15\text{--}20$ might be sufficient for a randomly homogeneously patterned world of points, but for some other underlying point patterns it would only yield a probability for one-connectivity a little above zero. For the random multifractal case, depicted in Fig. 5, the relative power has to be $P/P_{\text{norm}} \geq 40$ for this probability to come close to one, which corresponds to the numerically determined value $O(ngb) \geq 52$. Besides this sensitivity on the specific nature of the point patterns, also the target values $O(ngb) \approx 15\text{--}20$ and above are technologically unwanted, since they lead to too much blocking for the shared medium access control avoiding data-packet collision. The second drawback leads to frustration due to the specific nature of the bidirectional link definition. A cluster of spatially close-by nodes might saturate, meaning that each of the nodes has ngb neighbors. A new node, located not so far away from this cluster, wants to connect to some of its nodes. In fact, the nodes of the cluster are able to hear the lonely node due to its large transmission range, but since they are already saturated they do not increase their power to bridge the necessary spatial distance. The links are only one-directed, but not bidirected. Due to the missing feedback, the lonely node further increases its power, eventually up to its upper limit P_{max} , remaining in a frustrated state of having too few neighbors and unintentionally interfering the others' communication.

In order to avoid these drawbacks we present a modified local link rule. Upon setting up the communication links to the other nodes, a node attaches to its hello message information about its current link neighborhood list and its current transmission power. Starting with P_{min} , the node increases its transmission power by a small amount once it has not reached a minimum link degree ngb_{min} . Whenever another node, which so

far does not belong to the neighborhood list, hears the hello message of the original node for the first time, it realizes that the latter has too few neighbors, either sets its power equal to the transmission power of the hello-sending node or leaves it as before, whichever is larger, and answers the hello message. Now the original and new node are able to communicate back and forth and have established a new link. The original node adds one new node to its neighborhood list. Only once the required minimum link degree is reached, the original node stops increasing its power for its hello transmissions. At the end each node has at least ngb_{\min} neighbors. Some have more because they have been forced to answer nodes too low in ngb ; their transmission power is larger than necessary to obtain only ngb_{\min} neighbors for themselves.

Fig. 7 illustrates the algorithmic implementation of the local minimum-link-degree rule in more detail. Initially, all nodes come with a minimum transmission power $P_i = P_{\min}$ and an empty neighborhood list $\mathcal{N}_i = \emptyset$. All of them start in the receive mode. Then, at random, one of the nodes switches into the discovery mode. By subsequently sending hello messages and receiving hello replies, the picked node increases its power until it has discovered enough neighbors. Then the node returns into the receive mode. For simplicity we assume that only one node at a time is in the discovery mode; furthermore, we assume the maximum transmission power P_{\max} to be sufficiently large, so that each node is able to discover at least ngb_{\min} neighbors. Another node, which enters the discovery mode at a later time, performs the same operations. If during its previous receive-mode period this node had already been sending hello replies to then discovering nodes, it has to execute one more operation before returning into the receive mode: it compares its final discovery transmission power P_i^{disc} with the maximum power P_i it has been asked to transmit hello replies; if the former is smaller than the latter, the node updates its neighborhood list by sending a further hello message with the power $\max(P_i^{\text{disc}}, P_i)$ and receiving additional hello replies. In the receive mode a node listens to incoming hello messages. Upon receipt of such a message, the node first checks whether it already belongs to the incoming neighborhood list. If yes, the requesting node has already asked before with a smaller discovery power and there is no need for the receiving node to react. Otherwise, it updates its transmission power to $\max(P_i, P_j)$, but only if the magnitude of the incoming neighborhood list is smaller than the required minimum link degree. Then it sends back a hello reply. If the node in the receive mode has already executed its discovery mode before, an additional operation is needed to update its neighborhood list: it sends again a full hello message and listens to the newly triggered hello replies. Upon doing so, the node checks on the status of the initial hello reply, whether node j was able to receive it or not, and, if yes, makes sure that both nodes are registered in their mutual neighborhood lists. Also some hidden links are identified by this additional procedure; a hidden link occurs when two nodes, having already executed their discovery mode, are forced to increase their respective transmission powers by an independent third and fourth party in such a way, that they are then able to communicate directly to each other, but do not yet have this knowledge.

The implementation of the local minimum-link-degree rule written down in Fig. 7a represents the ad hoc node's view, which the latter use to selforganize into a network. The transmission power of each node is locally chosen to adapt to the spatial

```

(a)-LOCAL-MINIMUM-LINK-DEGREE-RULE_AD-HOC-NODE'S-VIEW()
1   $P_i \leftarrow P_{\min}$ 
2   $\mathcal{N}_i \leftarrow \emptyset$ 
3  RECEIVE-MODE()
4  DISCOVERY-MODE()
5  RECEIVE-MODE()
DISCOVERY-MODE()
1   $P_i^{\text{disc}} \leftarrow P_{\min}$ 
2   $\mathcal{N}_i^{\text{disc}} \leftarrow \emptyset$ 
3  while  $P_i^{\text{disc}} \leq P_{\max}$  and  $|\mathcal{N}_i^{\text{disc}}| < ngb_{\min}$ 
4      do  $P_i^{\text{disc}} \leftarrow P_i^{\text{disc}} \cdot (1 + \Delta)$ 
5          SEND-HELLO( $i, P_i^{\text{disc}}, \mathcal{N}_i^{\text{disc}}$ )
6          ( $j_1, i$ ), ...  $\leftarrow$  RECEIVE-HELLO-REPLYS()
7           $\mathcal{N}_i^{\text{disc}} \leftarrow \mathcal{N}_i^{\text{disc}} \cup \{j_1, \dots\}$ 
8   $P_i \leftarrow \max(P_i^{\text{disc}}, P_i)$ 
9  if  $P_i^{\text{disc}} < P_i$ 
10     then SEND-HELLO( $i, P_i, \mathcal{N}_i^{\text{disc}}$ )
11         ( $k_1, i$ ), ...  $\leftarrow$  RECEIVE-HELLO-REPLYS()
12          $\mathcal{N}_i \leftarrow \mathcal{N}_i^{\text{disc}} \cup \{k_1, \dots\}$ 
RECEIVE-MODE()
1  ( $j, P_j, \mathcal{N}_j$ )  $\leftarrow$  RECEIVE-HELLO()
2  if  $i \notin \mathcal{N}_j$ 
3      then if  $|\mathcal{N}_j| < ngb_{\min}$ 
4          then  $P_i = \max(P_i, P_j)$ 
5          SEND-HELLO-REPLY( $i, j$ )
6          if  $|\mathcal{N}_i| \geq ngb_{\min}$ 
7              then SEND-HELLO( $i, P_i, \mathcal{N}_i$ )
8              ( $k_1, i$ ), ...  $\leftarrow$  RECEIVE-HELLO-REPLYS()
9               $\mathcal{N}_i \leftarrow \mathcal{N}_i \cup \{k_1, \dots\}$ 

(b)-LOCAL-MINIMUM-LINK-DEGREE-RULE_SIMULATOR'S-VIEW()
1  for  $i \leftarrow 1$  to  $N$ 
2      do  $P_i \leftarrow P_{\min}$ 
3  for  $i \leftarrow 1$  to  $N$ 
4      do  $j(k) \leftarrow$  sort index  $1 \leq j \leq N, i \neq j$  in increasing order
5           $P_i \leftarrow \max(P_i, (r_{ij(ngb_{\min})})^\alpha)$ 
6          for  $k \leftarrow 1$  to  $ngb_{\min}$ 
7              do  $P_j \leftarrow \max(P_j, (r_{ij(k)})^\alpha)$ 

```

Fig. 7. Algorithmic implementations of the local minimum-link-degree rule: (a) the ad hoc node's view and (b) the simulator's view.

surrounding and is not globally assigned from outside. As simulators we employ an equivalent, but much simpler from-outside implementation. It is depicted in Fig. 7b. For each node i its relative distances r_{ij} to the other nodes j of the point pattern are sorted in increasing order. The first ngb_{\min} nodes of this list make up the discovery list $\mathcal{N}_i^{\text{disc}}$. Invoking (1), the discovery power $P_i = P_i^{\text{disc}} = (r_{ij(ngb_{\min})})^\alpha$ is fixed by the relative distance belonging to the ngb_{\min} 'th node of the sorted list, but needs to be updated according to $P_i = \max(P_i, (r_{ij})^\alpha)$ once the node i falls into the discovery neighborhood of the other nodes j . After completion of the heterogeneous power assignment, the links

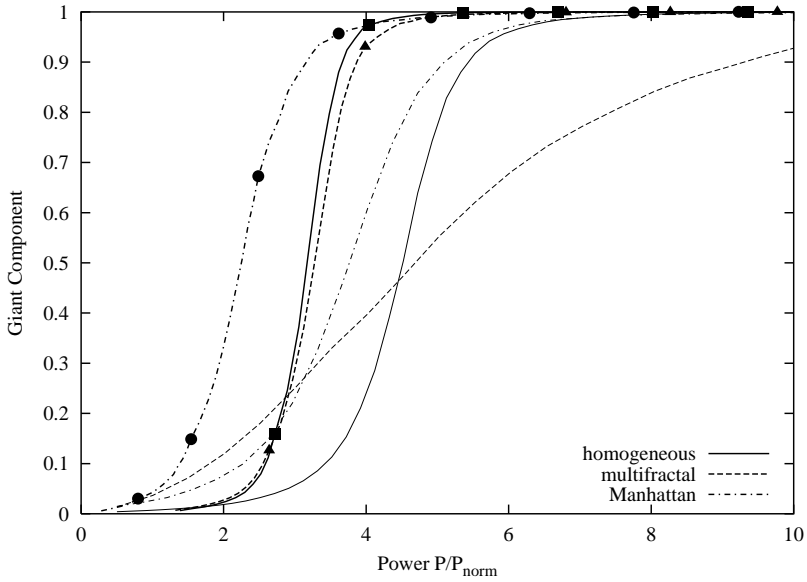


Fig. 8. Average relative giant component as a function of average transmission power upon using the local minimum-link-degree rule (curves with symbols) and the artificial constant- P rule (curves without symbols, identical to curves of Fig. 3). The number of nodes has been fixed to $N = 1600$ and the path-loss exponent has been set to $\alpha = 2$. Different line types of the curves correspond to different random spatial point patterns: homogeneous (solid), multifractal (dashed) with parameters $\beta = 0.4$ and $j = 5$, Manhattan (dash-dotted) with parameters $N_x = N_y = 7$; a sample of 500 geometric graphs has been used for each case. From the left to the right the symbols on each minimum-link-degree-rule curve stand for $ngb_{\min} = 2-7$ (homogeneous, multifractal) and $2-9$ (Manhattan).

are easily constructed along the lines of the definition given in Section 2.2, which then fix the final neighborhood lists \mathcal{N}_i .

4.2. Giant component and one-connectivity

Figs. 5 and 8 illustrate the simulation results obtained with the local minimum-link-degree rule and compares them to the respective outcomes of the artificial constant- P rule. For geometric graphs based on random homogeneous spatial point patterns the threshold of the average giant component is reduced by about a factor of 1.45; for the probability for one-connectivity the threshold reduction factor around 2.05 is even slightly larger. Note that for $ngb_{\min} = 3$ the relative giant component is already very close to one; once $ngb_{\min} \geq 6$ the probability for one-connectivity becomes one almost surely.

For geometric graphs based on random multifractal spatial point patterns the local minimum-link-degree rule beats the artificial constant P rule even more impressively. Whereas for the artificial rule the giant component threshold is very blurred, the local rule transforms it into a sharp threshold, which almost exactly coincides with the

respective threshold obtained for the previously discussed random homogeneous point patterns. Due to the strong spatial clustering the artificial constant- P rule leads to a highly suppressed one-connectivity yield; for the parameters used for Fig. 5 the onset for nonvanishing probability is already at a rather large transmission power around $P/P_{\text{norm}} \approx 13$, but it needs an even much larger P for this probability to come close to one. The local rule, on the other side, acts like a wondrous outperformer, compensating again the strong spatial clustering introduced by the inhomogeneous spatial point patterns and pushing the one-connectivity threshold down to $\langle P \rangle / P_{\text{norm}} \approx 6$, nearly matching the respective homogeneous-point-pattern threshold; with $ngb_{\text{min}} \approx 7$, which is equivalent to $\langle P \rangle / P_{\text{norm}} \approx 10$, the probability for one-connectivity is practically one.

In case of the geometric graphs based on random Manhattan spatial point patterns and in comparison with the artificial constant- P rule, the local minimum-link-degree rule reduces the threshold of the average giant component as well as of the probability for one-connectivity by about a factor of 1.7. The magnitude of reduction is comparable to the values stated for random homogeneous point patterns. For the one-connectivity probability to become almost one, a value of at least $ngb_{\text{min}} = 10$ is needed for the model parameters stated in Fig. 5.

4.3. Node degree and power transmission distribution

Next, we illustrate the node degree and transmission power distributions resulting from the minimum-link-degree rule and compare them with their constant- P counterparts. At first random homogeneous spatial point patterns are considered and the minimum link-degree is chosen to be $ngb_{\text{min}} = 6$ in order to guarantee one-connectivity almost surely; consult again Fig. 5. The node degree distribution $p(k)$, which reflects the probability for a node to have k neighbors, is shown in Fig. 9(a1). By construction, $p(k) = 0$ for $k < ngb_{\text{min}}$. It comes with a peak at $k = ngb_{\text{min}}$ and falls off sharply for $k > ngb_{\text{min}}$. Upon changing from discrete to continuous $k \geq ngb_{\text{min}}$, the distribution can be nicely fitted as the superposition $p(k) = a\delta(k - ngb_{\text{min}}) + bN(k; \mu, \sigma)$ of a δ -function, placed at the minimum link-degree, and a normalized Gaussian with shift μ and width σ . The parameters used for the fit in Fig. 9(a1) are $a = 0.14$, $b = 1.49$, $\mu = 5.93$ and $\sigma = 2.39$. For comparison we also show the much broader node degree distribution resulting from the constant- P rule. The setting $P/P_{\text{norm}} = 20$ is necessary to guarantee one-connectivity almost surely; consult again Fig. 5. This distribution can be nicely fitted with a normalized Gaussian; parameters used in Fig. 9(a1) are $\mu = 18.98$ and $\sigma = 4.92$. The small deviations to the expected Poissonian $p(k) = (\lambda^k/k!)e^{-\lambda}$ with mean $\lambda = P/P_{\text{norm}}$ (see Section 3.1), which is also illustrated in this Figure, are due to finite-size effects, that on average nodes close to the boundary experience a degree less than λ .

The power transmission distribution in case of the constant- P rule is simply a δ -function. It is indicated as an arrow within Fig. 9(a2). Its position naturally represents an approximate upper bound for power transmission values obtained from the minimum-link-degree rule. For the distribution resulting from the minimum-link-degree rule an analytic estimate can be given. For simplicity the path-loss exponent is set to $\alpha = 2$. As discussed already in Section 3.1, the degree distribution of a node,

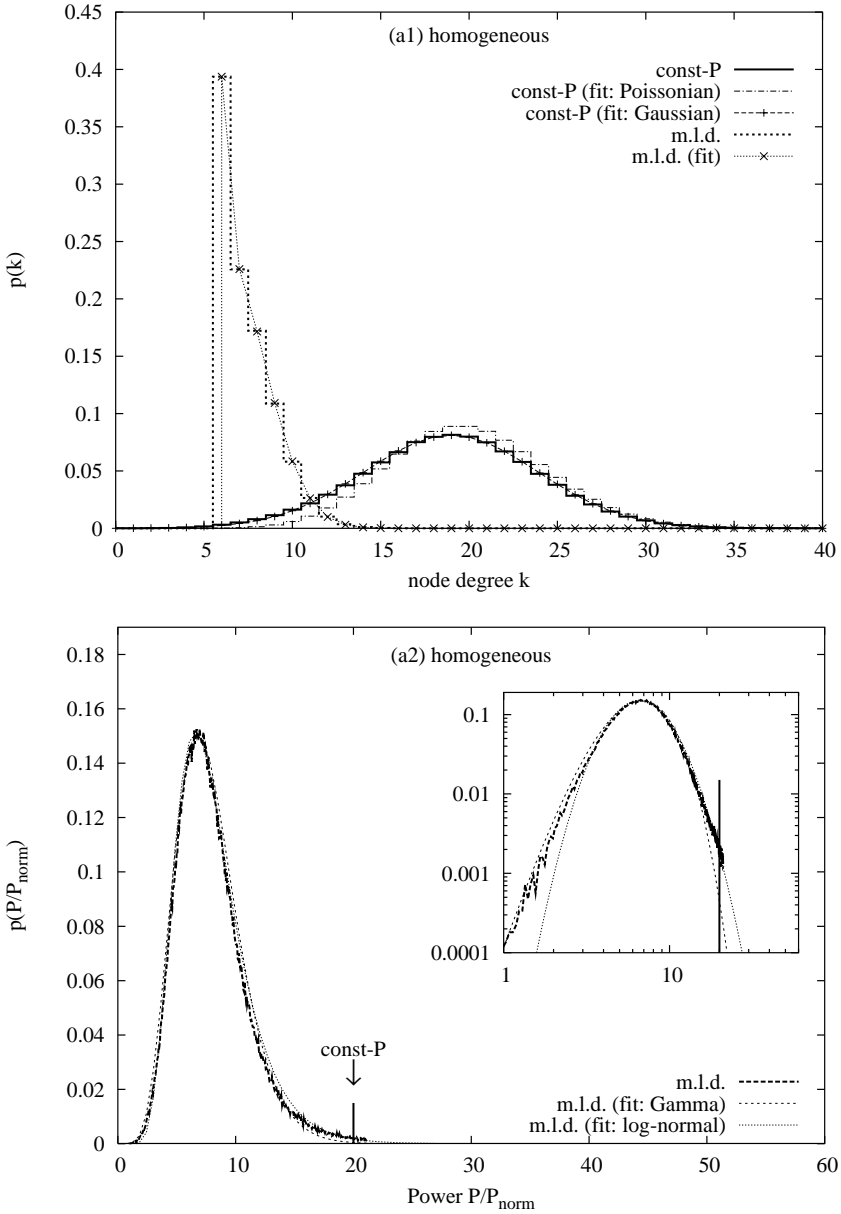


Fig. 9. Node degree and transmission power distributions obtained from the minimum link-degree (m.l.d.) and the constant- P rule. Details about the fitted distributions are given in the main text. The number of nodes has been fixed to $N = 1600$ and the path-loss exponent has been set to $\alpha = 2$. Different random spatial point patterns are used: homogeneous (a), multifractal (b) with parameters $\beta = 0.4$ and $j = 5$, and Manhattan (c) with parameters $N_x = N_y = 7$; a sample of 500 geometric graphs has been used for each case.

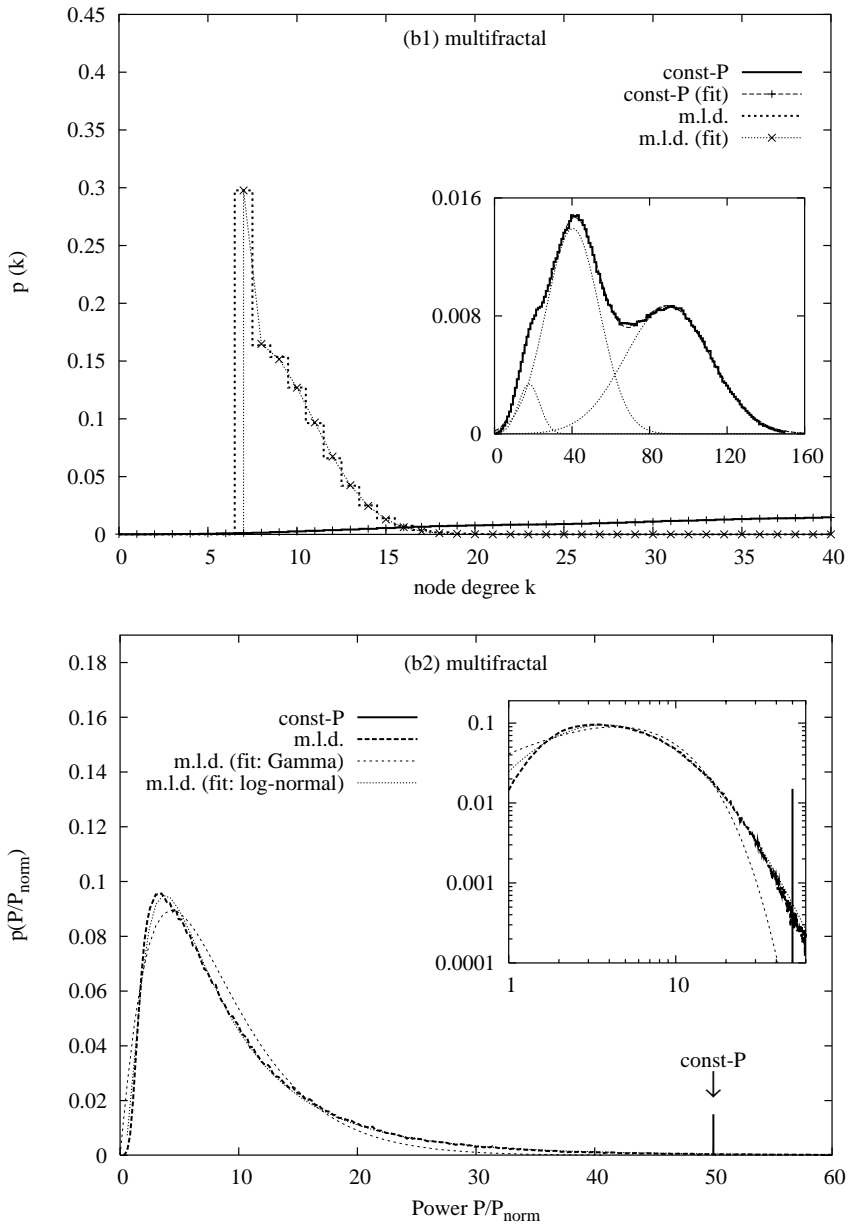


Fig. 9. Continued.

not too close to a boundary, is given by the Poissonian $p(k) = (qN)^k e^{-qN}/k!$, with $q = (P/P_{\text{norm}})(\pi R_{\text{norm}}^2/L^2) = (P/P_{\text{norm}})/N$ representing the area covered by the node's transmission radius relative to the total domain area $L^2 = 1$. Here, the transmission power P is kept fixed and the degree k is the discrete random variable. Another

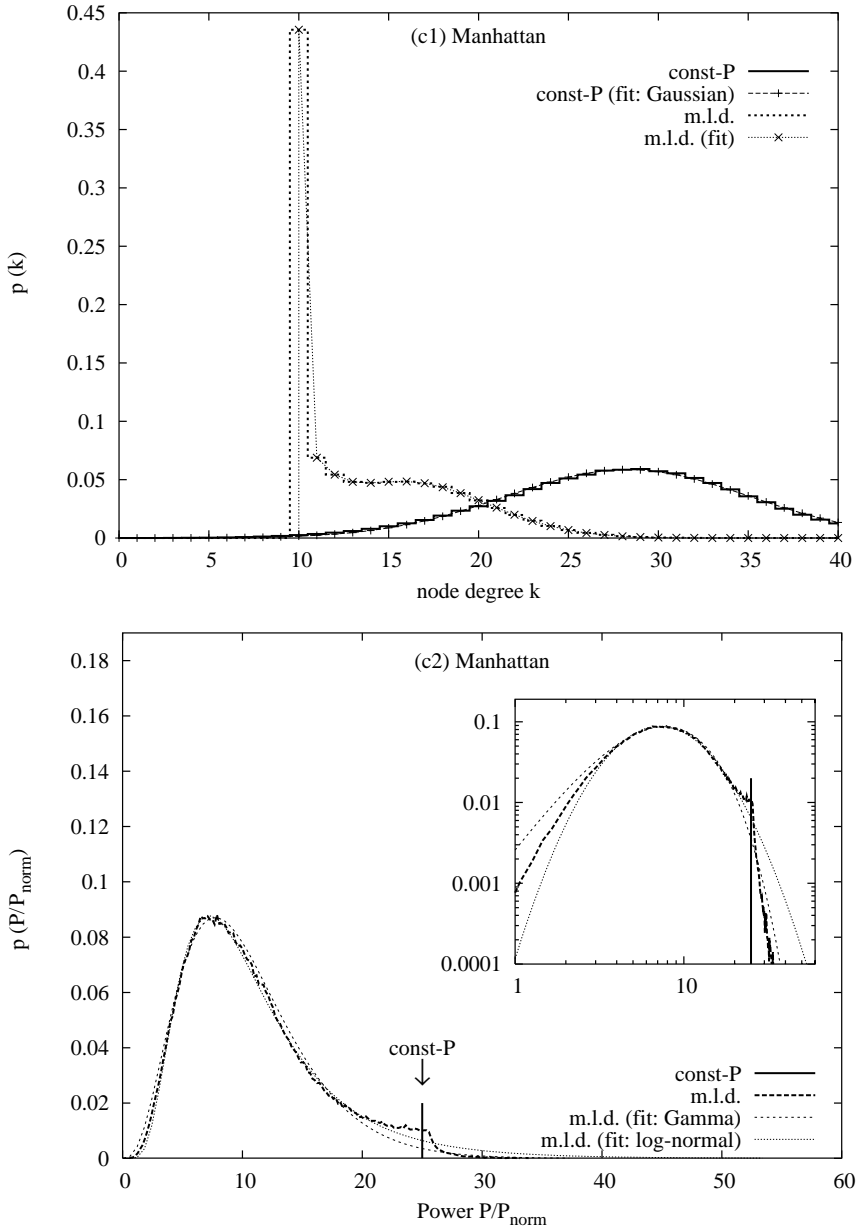


Fig. 9. Continued.

look on Fig. 9(a1) reveals, that the very narrow degree distribution resulting from the minimum-link-degree rule can be crudely approximated as $p(k) \approx \delta(k - k_0)$ with $k_0 = \langle k \rangle = 7.36$. Hence, the node degree is now kept fixed within the above Poissonian and the transmission power is considered as the continuous random variable. This leads

to the transmission power distribution

$$p(P/P_{\text{norm}}) \sim (P/P_{\text{norm}})^{k_0} \exp(-P/P_{\text{norm}}). \quad (4)$$

It corresponds to a Gamma distribution $p(x; a, b) = x^{a-1} e^{-x/b} / (b^a \Gamma(a))$ with $x = P/P_{\text{norm}}$ and $a = k_0 + 1 \approx 8.36$, $b = 1$. The actual best fit to the sampled distribution, shown in Fig. 9(a2), yields the parameters $a = 7.74$, $b = 1.01$ and more or less confirms the given estimate. A fit with a lognormal distribution $p(x) = \exp\{-(\ln x - \mu)^2 / 2\sigma^2\} / (\sqrt{2\pi}\sigma x)$ is also illustrated; parameter values are $\mu = 2.02$ and $\sigma = 0.37$.

Node degree and transmission power distributions in connection with random multifractal spatial point patterns are illustrated in Figs. 9(b1) and (b2). The minimum link-degree rule produces a node degree distribution, which as for the homogeneous example can be nicely approximated by a superposition of a δ -function and a normalized Gaussian for $k \geq ngb_{\text{min}} = 7$. The parameters used for the fit in Fig. 9(b1) are $a = 0.13$, $b = 1.36$, $\mu = 7.60$ and $\sigma = 3.27$. For comparison, the node degree distribution obtained from the constant- P rule is also illustrated. In order to guarantee one-connectivity almost surely, a rather large $P/P_{\text{norm}} = 50$ has to be picked. This leads to a very broad distribution, which comes with an average degree $\langle k \rangle = 62.7$ and which can be represented as a superposition $p(k) = a_1 N(k; \mu_1, \sigma_1) + a_2 N(k; \mu_2, \sigma_2) + a_3 N(k; \mu_3, \sigma_3)$ of three normalized Gaussians with parameters $a_1 = 0.04$, $\mu_1 = 17.8$, $\sigma_1 = 5.5$, $a_2 = 0.48$, $\mu_2 = 40.4$, $\sigma_2 = 13.7$, $a_3 = 0.48$, $\mu_3 = 89.5$, $\sigma_3 = 22.0$. The occurrence of the double-hump structure is specific to the chosen parameters $N = 1600$, $\beta = 0.4$ and $P/P_{\text{norm}} = 50$, where the transmission range area associated to the transmission power smoothes out any substructure generated beyond the iteration step $j \approx 2-3$ of the multifractal point pattern construction. The sampled transmission power distribution resulting from the minimum link-degree rule is exemplified in Fig. 9(b2). A best fit to a Gamma and a lognormal distribution reveals better agreement with the latter. Best parameters are $a = 2.11$, $b = 3.94$, and $\mu = 1.97$, $\sigma = 0.81$, respectively.

For completeness, node degree and transmission power distributions in connection with random Manhattan spatial point patterns are illustrated in Figs. 9(c1) and (c2). The choice $P/P_{\text{norm}} = 25$ guarantees one connectivity almost surely in context with the constant- P rule and leads to a rather broad Gaussian-like node degree distribution. The corresponding curve in Fig. 9(c1) comes with mean $\mu = 28.3$ and width $\sigma = 6.8$. Note, that the transmission radius corresponding to $P/P_{\text{norm}} = 25$ equals about half the length $1/N_x = 1/N_y$ of a Manhattan block, so that the influence of the Manhattan structure still impacts the node degree distribution and has not been washed out to coincide with a node degree distribution of a random homogeneous point pattern with $\mu \approx 25$. This difference also holds for the node degree distribution resulting from the minimum link-degree rule. The peak at $k = ngb_{\text{min}} = 10$ is very pronounced. The overall mean is $\langle k \rangle = 13.53$ and the distribution $p(k \geq ngb_{\text{min}}) \approx a\delta(k - ngb_{\text{min}}) + b_1 N(k; \mu_1, \sigma_1) + b_2 N(k; \mu_2, \sigma_2)$ can be approximated as a superposition of a δ -function and two normalized Gaussians. Parameters used in Fig. 9(c1) are $a = 0.35$, $b_1 = 0.63$, $\mu_1 = 7.78$, $\sigma_1 = 2.31$, and $b_2 = 0.56$, $\mu_2 = 15.90$, $\sigma_2 = 4.60$. The sampled transmission power distribution resulting from the minimum link-degree rule is exemplified in Fig. 9(c2). A best fit to a Gamma and a lognormal distribution reveals a slightly better

agreement with the latter, but deviations from both are clearly visible. Best parameters are $a = 4.00$, $b = 2.57$, and $\mu = 2.27$, $\sigma = 0.54$, respectively.

5. Conclusion

For wireless mobile ad hoc communication networks connectivity represents an important issue. In a selforganizing manner, the participating ad hoc nodes have to tune their transmission powers to establish direct one-hop communication links to their spatial neighbors and to be able to reach all others via multihop routes. In the static limit, two-dimensional continuum percolation based on discs with constant or random radius can be mapped onto artificial link coordination rules with constant or random transmission power. Basically the transmission powers have to be chosen above a percolation threshold in order to guarantee strong network connectivity almost surely. However, the percolation threshold does show a sensitive dependence on the specific spatial patterning of the ad hoc nodes. Different classes of uncorrelated and correlated random point patterns, like homogeneous, multifractal or Manhattan-like distributions, make a big difference. The artificial link rules are not flexible enough to adapt to local spatial inhomogeneities. A local generalization of these rules leads to the minimum-link-degree rule. It can be viewed as a step towards a selforganizing mutation of continuum percolation. It requires each ad hoc node to be connected to a minimum number of closest neighbors, which sets a lower bound on the node's transmission power. This node, on the other hand, might be forced to increase its transmission power further, in order to establish an additional communication link to another node, which belongs to the greater vicinity and has not yet reached the required minimum number of closest neighbors. This distributed rule is able to counterbalance local spatial inhomogeneities occurring in the random point patterns. As a function of average transmission power the percolation thresholds associated to the various considered classes of random point patterns almost collapse onto each other and are tremendously reduced, when compared to the outcomes with the artificial rules.

Compared to other local link rules yielding strongly connected networks, the presented minimum-link-degree rule is simple. For example, the Rodoplu and Meng algorithm [32] relies on GPS-based position knowledge of the ad hoc nodes to construct a link enclosure for each node; the construction also requires knowledge about the assumed uniform path-loss exponent, which can be seen as another drawback of this algorithm. Another proposal [33] requires ad hoc nodes to come with directional antennas; strong network connectivity is then guaranteed once each node has neighbors in each angular sector. Rules like these require more technological equipment for the ad hoc nodes. In terms of the simplicity principle, the presented minimum-link-degree rule appears to be more attractive. It also has the advantage that it will work in a heterogeneous propagation medium, where the path-loss exponent is a function of position, distance and direction. A generalization of the distributed minimum-link-degree rule, which so far only has been developed for the static limit, towards mobile ad hoc networks is straightforward. These last two issues will be discussed in more detail in future work.

Finding efficient distributed coordination rules, i.e., protocols, for connectivity is certainly one important issue for ad hoc communication networks, but there are definitely also others: power consumption, efficient routing discovery and execution, medium access control, interference, quality of service, and end-to-end throughput. The construction of an optimized protocol for one part alone, needs not be the overall best for all of the partially conflicting entities considered together. Clearly, the design of a rather complex, but still simple overall protocol is called for. It is possible that such an optimized protocol might lead to small-world or scale-free geometric-graph topologies, which are already observed and discussed for Internet and biochemical communication networks [34,35].

Acknowledgements

The authors acknowledge fruitful discussions with Michael Bahr, Rainer Sauerwein, Clemens Hoffmann and Bernd Schürmann. W.K. acknowledges support from the Ernst von Siemens-Scholarship.

References

- [1] J.G. Proakis, *Digital Communications*, McGraw-Hill, Singapore, 1995.
- [2] R. Prasad, *Universal Wireless Personal Communications*, Artech House, Boston, 1998.
- [3] T.S. Rappaport, *Wireless Communications—Principles & Practice*, Prentice Hall, Upper Saddle River, 1999.
- [4] Z.J. Haas, et al. (Eds.), Special issue on wireless ad hoc networks, *IEEE J. Select Areas Commun.* 17(8) (August 1999).
- [5] J.P. Hubaux, T. Gross, J.Y. Le Boudec, M. Vetterli, Toward Self-Organized Mobile Ad Hoc Networks: The Terminodes Project, *IEEE Communications Magazine*, January 2001.
- [6] Mobile Ad Hoc Networks (manet) Working Group, <http://www.ietf.org/html.charters/manet-charter.html>.
- [7] Wireless Ad Hoc Networks Bibliography, http://w3.antd.nist.gov/wctg/manet/manet_bibliog.html.
- [8] R. Meester, R. Roy, *Continuum Percolation*, Cambridge University Press, Cambridge, 1996.
- [9] D. Stoyan, W.S. Kendall, J. Mecke, *Stochastic Geometry and its Applications*, Wiley, Chichester, 1995.
- [10] J. Dall, M. Christensen, arXiv:cond-mat/0203026.
- [11] D.R. Baker, G. Paul, S. Sreenivasan, H.E. Stanley, arXiv:cond-mat/0203235.
- [12] M.B. Isichenko, *Rev. Mod. Phys.* 64 (1992) 961.
- [13] P. Blanchard, G. Dell'Antonio, D. Gandolfo, M. Sirugue-Collin, *J. Stat. Phys.* 106 (2002) 1.
- [14] J. Feder, *Fractals*, Plenum Press, New York, 1988.
- [15] U. Frisch, *Turbulence*, Cambridge University Press, Cambridge, 1995.
- [16] C. Meneveau, K.R. Sreenivasan, *J. Fluid Mech.* 224 (1991) 429.
- [17] M. Greiner, J. Gieseemann, P. Lipa, P. Carruthers, *Z. Phys. C* 69 (1996) 305.
- [18] M. Greiner, H. Eggers, P. Lipa, *Phys. Rev. Lett.* 80 (1998) 5333.
- [19] T. Lux, *Quant. Finance* 1 (2001) 632.
- [20] J.F. Muzy, J. Delour, E. Bacry, *Eur. Phys. J.* 17 (2000) 537.
- [21] V.J. Ribeiro, R.H. Riedi, R.G. Baraniuk, Wavelets and Multifractals for Network Traffic Modeling and Inference, Proceedings of the ICASSP, Salt Lake City, Utah, May 7–11, 2001.
- [22] E.A. De Wolf, I.M. Dremmin, W. Kittel, *Phys. Rep.* 270 (1996) 1.
- [23] T. Halsey, M. Jensen, L. Kadanoff, I. Procaccia, B. Shraiman, *Phys. Rev. A* 33 (1986) 1141.
- [24] B. Bollobás, *Random Graphs*, Academic Press, London, 1985.
- [25] D.R. White, M.E.J. Newman, Santa Fe Institute working paper 01-07-035.

- [26] M.D. Penrose, *Random Structures and Algorithms* 15 (1999) 145.
- [27] P. Gupta, P.R. Kumar, *IEEE Trans. Inf. Theory* IT-46 (2000) 388.
- [28] D. Stauffer, A. Aharony, *Introduction to Percolation Theory*, Taylor & Francis, London, 1992.
- [29] O. Dousse, P. Thiran, M. Hasler, presented at IEEE INFOCOM 2002, New York, June 23–27, 2002, <http://www.ieee-infocom.org/2002/papers/481.pdf>.
- [30] M.K. Marina, S.R. Das, Routing Performance in the Presence of Unidirectional Links in Multihop Wireless Networks, in *Proceedings of the Third ACM International Symposium on Mobile Ad Hoc Networking and Computing (MOBIHOC 2002)*, Lausanne, Switzerland, June 9–11, 2002, pp. 12–23.
- [31] R. Ramanathan, R. Rosales-Hain, Topology Control of Multihop Wireless Networks using Transmit Power Adjustment, *Proceedings of the IEEE INFOCOM 2000* (March 2000).
- [32] V. Rodoplu, T.H. Meng, *IEEE J. Select. Areas Commun.—Special Issue on Ad Hoc Networks* 17 (1999) 1333.
- [33] L. Li, J. Halpern, P. Bahl, Y. Wang, R. Wattenhofer, arXiv:cs.NI/0209012.
- [34] R. Albert, A.L. Barabasi, *Rev. Mod. Phys.* 74 (2002) 47.
- [35] S.N. Dorogovtsev, J.F.F. Mendes, *Adv. Phys.* 51 (2002) 1079.